Coastal Carolina University
CCU Digital Commons

Electronic Theses and Dissertations | College of Graduate Studies and Research

12-31-2016

An Ensemble Study of the Sea Level Rise Impact on Storm Surge and Inundation in the Coastal Bangladesh

Mansur Ali Jisan
Coastal Carolina University

Follow this and additional works at: https://digitalcommons.coastal.edu/etd

 Part of the Climate Commons

Recommended Citation
Jisan, Mansur Ali, "An Ensemble Study of the Sea Level Rise Impact on Storm Surge and Inundation in the Coastal Bangladesh" (2016). *Electronic Theses and Dissertations*. 24.
https://digitalcommons.coastal.edu/etd/24

This Thesis is brought to you for free and open access by the College of Graduate Studies and Research at CCU Digital Commons. It has been accepted for inclusion in Electronic Theses and Dissertations by an authorized administrator of CCU Digital Commons. For more information, please contact commons@coastal.edu.

An Ensemble Study of the Sea Level Rise Impact on Storm Surge and Inundation in the Coastal Bangladesh

By

Mansur Ali Jisan

Submitted in Partial Fulfillment of the

Requirements for the Degree of Master of Science in

Coastal Marine and Wetland Studies in the

Department of Coastal and Marine Systems Science

Coastal Carolina University

2017

Dr. Shaowu Bao	Dr. Leonard J. Pietrafesa
Major Professor	Committee Member
Dr. Varavut Limpasuvan	Dr. Michael Roberts
Committee Member	Dean, College of Science
Dr. Richard F. Viso	
Director of CMSS	

© Copyright

Mansur Ali Jisan, 2017

All Rights Reserved

DEDICATION

To my parents for the gift of life

and to my wife for her continuous love & support throughout this journey.

ACKNOWLEDGEMENTS

This work would never be possible without the support from my advisor Dr. Shaowu Bao and co-advisors Dr. Len Pietrafesa and Dr. Var Limpasuvan. I wholeheartedly thank them for their continuous support, motivation and guidance.

I thank Dr. Bao for his constant support as a mentor, teacher, colleague and foremost, as a friend. Whenever I needed any advice either academic or non-academic, I always looked upon him. He very patiently critiqued my research methods and allowed me to develop an independent research approach which I will always cherish. At this stage of my academic life, I feel more well-organized, modest and confident after working under his guidance. I feel lucky to get the opportunity to discuss various topics related to coupled air-sea process and coastal hydrodynamics with Dr. Pietrafesa. His way of analysis and interpretation fashioned my way of thought in problem solving. My experience working with him will always be an asset. I feel privileged to learn from the knowledgeable professors: Roi Gurka, Eric Koepfler, Louis Keiner, Thomas Mullikin, Erin Hackeett, Rich Viso and Till Hanebuth. I thank them for imbibing me with the knowledge required to study coastal processes. I wish to thank Joseph Baxley and Dr. Mike Murphy from the Cyber-infrastructure project for their continuous help in solving problems regarding the High-performance computing works. I would like to extend my thanks to Karen Fuss, Julie Quinn, Glenda Kelley and Coastal Carolina University's Office of International Programs for their supports regarding the administrative issues and immigration related works.

Special thanks to my friends Lukas, Dongliang, Hongyuan, Akim, Krishnan, Jiarong, Todd, Sam, Austin for sharing the sweetness of friendship and for all the entertaining conversations. I'm also thankful to my friends from my 'Climate Reality' and 'Climate Activists Bangladesh' family for their regular discussion about Climate Change policies which really kept me motivated to study about Earth-Ocean-Atmosphere Sciences. I wish all the best for you in future endeavors. Finally, I thank my wife Nadia for sharing all the joy & love and her endless support during the difficult times throughout this journey.

ABSTRACT

The hydrodynamic model Delft3D is used to study the impact of Sea Level Rise (SLR) on storm surge and inundation in the coastal region of Bangladesh. To study the present-day inundation scenario, track of two known tropical cyclones (TC) were used: Aila (Category 1; 2009) and Sidr (Category 5; 2007). Model results were validated with the available observations. Future inundation scenarios were generated by using the strength of TC Sidr, TC Aila and an ensemble of historical TC tracks but incorporating the effect of SLR.

Since future change in storm surge inundation under SLR impact is a probabilistic incident, that's why a probable range of future change in inundated area was calculated by taking in to consideration the uncertainties associated with TC tracks, intensities and landfall timing. Along with that, role of topographic slope was investigated to see how they could alter the impact of SLR on storm surge and inundation.

The model outputs showed that, the inundated area for TC Sidr, which was calculated as 1860 km^2, would become 31% higher than the present-day scenario if a SLR of 0.26 meter occurs during the mid-21st century climate scenario. Similar to that, an increasing trend was found for the end of the 21st century climate scenario. It was found that with a SLR of 0.54 meter, the inundated area would become 53% higher than the present-day case.

Along with the inundation area, the impact of SLR was examined for the changes in future storm surge level. A significant increase of 21% was found in storm surge level for the case of TC Sidr in Barisal station if a Sea Level Rise of 0.26 meter occurs at the middle of the 21st century. Similar to that, an increase of 37% was found in storm surge level with a SLR of 0.54 meter in this location for the end of the 21st century climate scenario.

Ensemble projections based on uncertainties of future TC events also showed that, for a change of 0.54 meters in SLR, the inundated area would range between 3500-3750 km^2 whereas for present day SLR simulations it was found within the range of 1000-1250 km^2

Outputs from the topographic slope-storm surge inundation experiments showed that, even coastal areas with a steep topographic slope, inundated area would increase greatly due to the impact of SLR.

These results revealed that even if the future TCs remain at the same strength as at present, the projected changes in SLR will generate more severe threats in terms of surge height and extent of inundated area.

TABLE OF CONTENTS

LIST OF TABLES

LIST OF FIGURES

1. INTRODUCTION

Five basic processes (i.e., atmospheric pressure, the direct wind forcing, the earth's rotation, surface gravity waves and rainfall) cause water level rise under storm conditions (Harris et al., 1963). Pietrafesa *et al.* (1986) also pointed a *non-local* process in which high water at the mouths of coastal estuaries, bays and rivers can block discharges of upstream waters and contribute to upstream flooding. Among these processes, storm surges form primarily due to Tropical Cyclone (TC) wind stresses mechanically driving the surface frictional layer onshore. Assuming an idealized balance between the pressure gradient force and the surface wind stress with a small bottom stress, the surge related to TC wind stress can be expressed as $\Delta h = \frac{t_w L}{g \rho h}$, where L is the fetch of the wind (the distance over which the wind blows), τ_w is the wind stress due to the friction between the moving air and water surface, g is the gravity, ρ is the density of water, and h is the normal water depth near the coast (Hearn, 2008). Also as a secondary process, due to the differences in atmospheric pressure level, the water level rises in the areas of low atmospheric pressure and falls in the areas of high atmospheric pressure, which is how the rising water level offsets the low atmospheric pressure to keep the total pressure constant (Harris *et al*., 1963). Of course, it is possible that the entirety of the local region under study could be smaller than that of the spatial dimension of the low-pressure storm system, and in that case, all of

the water surface would be subjected to lower pressure and thus not display any gradients in kind.

Bangladesh has a long history of devastation due to coastal storm surges. The coastal part of Bangladesh is frequently flooded by storm surges induced by TCs, in addition to routine inundation from upstream river water and the downstream tides. The Bay of Bengal is a very active area for the development of TCs (Figure 1). Typically, TC-induced storm surges in this area originate in the central or southern part of the Bay of Bengal or near the Andaman Sea. The average annual number of tropical depressions in the Bay of Bengal is around 12 with about five attaining hurricane strengths. Most of the Bay of Bengal cyclones make landfall on the eastern coasts of India and Sri Lanka, and on the coasts of Bangladesh and Myanmar. The southwest monsoon plays an important role in the cyclone development, and cyclones usually occur either in the pre-monsoon months (April to June) or the post-monsoon months (October to December). Based on TC activity between 1877 to 1998, Singh *et al*. (2001) concluded that both the intensity of and frequency of TCs tend to maximize during November, the post-monsoon period. McPhaden *et al.* (2009) and Sengupta *et al.* (2008) attribute this tendency to the two prevailing atmospheric conditions during this period: 1) thermodynamic instability and weak vertical wind shear and 2) formation of stratified upper ocean layers. These two conditions couple to create the primary reasons behind this high TC activity during the post-monsoon period.

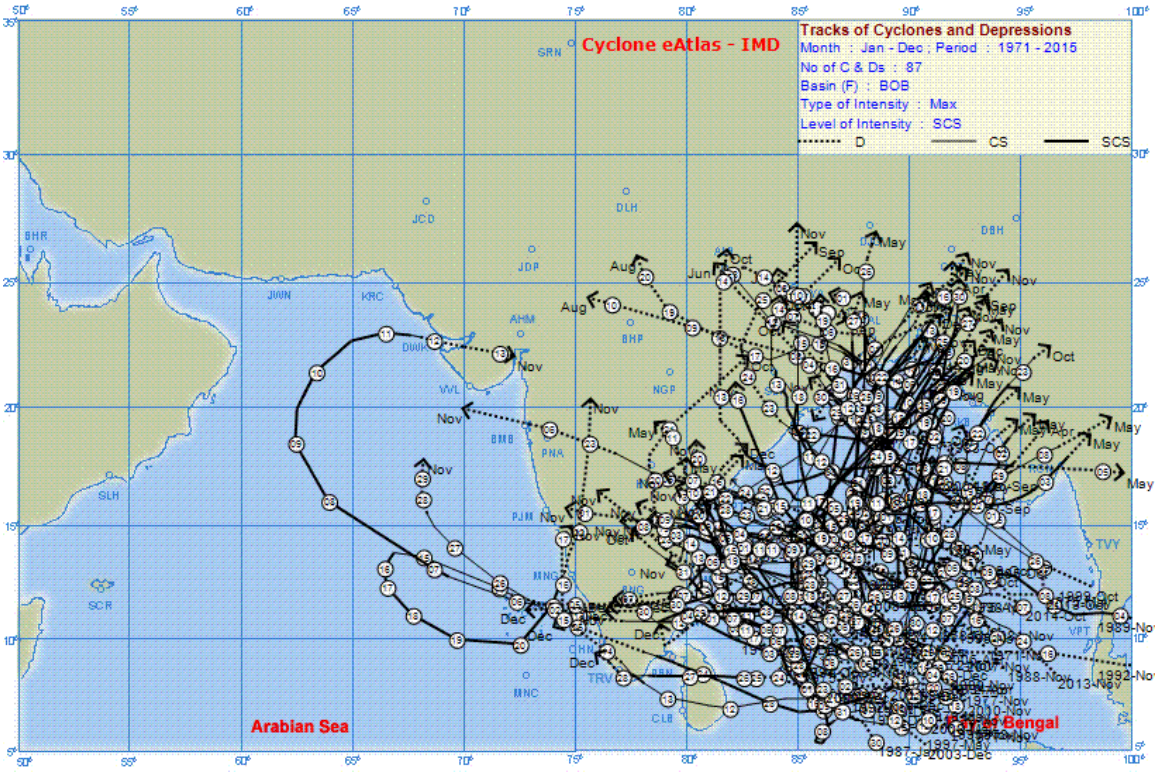

Figure 1: Historical Severe Cyclonic Storms (Indian Meteorological Department **(**IMD) scale) over Bay of Bengal for the period of 1971 till 2015.

Even though only 5-6% of the global cyclones form in this region, those that do can be very deadly. As a result, 80-90% of cyclone-induced global losses in terms of lives and property are experienced in this region (Chowdhury, 2002), and 15 of the top 20 deadliest cyclones in the recorded history developed in the Bay of Bengal. Nicholls *et al*. (1995) reported that about 42% of TC associated human life loss has occurred in Bangladesh during the last two centuries. In most cases, the main reason for this large-scale death and destruction is storm surge and inundation (Chowdhury *et al.* 1993; Ikeda 1995). According to the South Asian Association for Regional Cooperation (SAARC) Meteorological Research Center (SMRC, 2008), the highest level of storm surge recorded in Bangladesh was 13 m. Since 1970, four severe cyclones with maximum wind speeds greater than 61 m

s^{-1} and storm surges over 4 meters have hit Bangladesh, in November 1970, April 1991, May 1997 and November 2007, respectively (Karim *et al.*, 2008). Because of the relatively shallow coastal-inland topography, storm surge induced inundation has occasionally reached 60 km inland from the coast (Chowdhury, 2003).

Several factors contribute to the vulnerability of the Bangladesh coastal region to TC-induced storm surges and inundation. The geomorphological characteristics of the Bangladesh coastal region have made the locale prone to major TC events. The process of riverine sedimentation has formed most of the areas near the coastal zone of Bangladesh. As such, the low-lying areas are relatively flat and, thereby, susceptible to flooding even under normal astronomical tide conditions. Furthermore, the triangular shape of the Bay of Bengal region tends to funnel water inland, exacerbating the effects of storm surges. For example, the concave shape of the bay, a funnel-shaped convergence toward the Meghna estuary, the existence of a very wide continental shelf, a large astronomical tidal range, a complex coastline, and high volumetric river discharges from land are amongst the regional physical features (Ahmed and Falk 2008; Chowdhury 2002; Shamsuddoha and Chowdhury 2007). Second, according to Murty et al. (1986), storm surges amplify vertically as they approach the coast due to the shallow continental shelf of the Bay of Bengal, which causes massive flooding in the low-lying coastal areas where a large percentage of the Bangladesh population resides. Third, the relatively high losses of human life and property could also be related to the high population density in the low-lying coastal areas of Bangladesh. In addition, the socio-economic condition of coastal residents contributes to the vulnerability of people and property to cyclones, as most of the residents in the coastal areas are relatively poor and thus live in inadequately constructed houses that are not strong enough

to withstand the strong wind and storm surges (Chowdhury *et al.* 1993). Finally, the high tidal ranges in the northern Bay of Bengal might also be responsible for the large-scale destruction, especially when the surges occur at the time of high tide. Due to the relatively higher tidal range, the effect of storm surge becomes far more severe when it occurs in concert with a high astronomical tide. In summary, due to the above-mentioned factors, these coastal flood events associated with the changes in coastal water level due to storms passing over the sea cause great loss to human lives, property, livelihoods and the economy of the country (Haque, 1997). Bangladesh has experienced such incidents several times in the past (Institute of Water Modeling, 2005), including the 1970 Bhola cyclone, which caused a highest water level of 10 m above MSL during high spring tide, thus resulting in large-scale inundation to the low-lying coastal area (Karim *et al.*, 2008; SMRC 1998).

Future climate change may increase the threats of TC-induced storm surge and inundation. According to the Intergovernmental Panel on Climate Change Fourth Assessment Report (IPCC 4AR), there is a high probability of major changes in TC activity across various ocean basins including the Arabian Sea and the Bay of Bengal. According to Milliman *et al.* (1989), the Ganges-Brahmaputra-Meghna Delta region has long been characterized as a highly vulnerable zone due to its exposure to the increasing trend of sea level rise (SLR). According to the SLR analysis done by the SAARC based on the 22-year record of the observed sea level at Charchanga, Cox's Bazar and Hiron Point, sea level is rising at the rates of 6.0, 7.8 and 4 mm $year^{-1}$, respectively, in those three locations (SMRC, 2003). These rates are much higher than the global average rate of SLR (~ 3.2 mm/year) over the last 25 years (Pietrafesa *et al.*, 2016). Based on Warrick *et al.* (1996), the sea level in the Bay of Bengal is also influenced by local factors including tectonic setting, deltaic

processes and sediment load. For example, the coastal region of Bangladesh has been subsiding due to the pressure on the Earth's crust from the sediment with thick layers that has formed over millions of years. Warrick *et. al.* (1996) also analyzed the recent history of land accretion and suggested that the subsidence is also balanced by land accretion due to sediment supply from the coast. These physical phenomena have been shaping the coast of Bangladesh over the past 100 years. A global SLR of 26-59 cm over the rest of the century has been projected by the IPCC under the scenario A1F1 (Meehl *et al.* 2007). In this proposed work, we will use the suggested SLR projection of Caesar *et al.* (2017, under review) to examine the effect on the Bangladesh coastal. This project is 26 cm for the mid-21st century (2040 -2060) and 54 cm for the end-21st century (2079 -2099)

Previous studies have analyzed the likely impact of climate change, especially SLR, on storm surge and inundation in this region. Using hydrodynamic models, Ali (1992) showed that with an increase of 1.0 and 1.5 meters of SLR, 10% and 15.5%, respectively, of the entirety of Bangladesh would get flooded under the strength of future TCs. Karim and Mimura (2008) used a 1-D hydrodynamic model to study the future TC-induced coastal inundation under several of climate change scenarios by changing sea surface temperature (SST), SLR, wind speed and sea level pressure. These authors concluded that with an increase of 2^{o}C in SST and 0.3 meters of SLR, the flood risk area would be 15.3% more than the present-day risk area, and the depth of flooding would increase by as much as 22.7% within 20 km from the coastline.

Both Ali (1992) and Karim & Mimura (2008) considered SST rise and future strength of TCs in simulating the future storm surge and inundation. However, the impact of climate change on the frequency and intensity of TCs are still debatable (Knutson *et al*., 2010). The

projection of the TC characteristics in the Bay of Bengal region is likewise unclear. To address these uncertainties, a reasonable method to examine the impact of future SLR on storm surge and inundation would be to construct an ensemble of tracks and intensities of possible future landfalling TCs along the Bangladesh coast based on the historical TC records. Using this statistical approach, we can quantify the impact of future SLR on coastal storm surge and inundation caused by the statistically probable TC tracks in the future. To date, such an approach has not been taken and will be a focus of this study. In addition, we hypothesize that the coastal topography, especially its slope (that is the rise over run), could alter the impact of future SLR on storm surge and inundation. We will test this hypothesis by simulating the impact of future SLR on storm surge and inundation for different coastal topographic characteristics. Results of this investigation will provide useful information and guidance for other coastal regions.

We first will use the Delft3D community numerical model to simulate the present-day storm surge and inundation using the strength of two recent TCs (TC Sidr and TC Aila), and validate the simulations with observational data. Using the validated setup of the model, future storm surge and inundation scenarios will then be generated by incorporating the projected SLR, ensemble of TC tracks from historical datasets, and a variety of topographic slopes.

The study will be carried out in the Ganges-Brahmaputra-Meghna Delta regions (Figure 2). According to the Integrated Coastal Zone Management Plan, 19 districts of Bangladesh located near the Bay of Bengal area have been defined as the coastal areas, which are all included in the study domain (Figure 2). As mentioned earlier, we selected two TC cases in this study for validation purposes: the strong Saffir-Simpson (SS) Category-5 TC Sidr

that directly hit the study area and the SS Category-1 TC Aila that made landfall in the South-West part of the study domain. TC Sidr made landfall near Barguna district (Fig. 2) in 2007 and caused ~ 3000 human fatalities and leaving millions homeless. TC Aila occurred in the Bay of Bengal region in the year 2009 and, although a category-1 storm, caused ~ 190 deaths and affected 4.8 million people, a devastation that left a long-term impact. The locales mainly affected were Khulna, Patukhali and Chandpur. The storm surge due to Aila broke a dam in Pataukhali and submerged five villages, destroying huge number of homes and leaving thousands of people homeless.

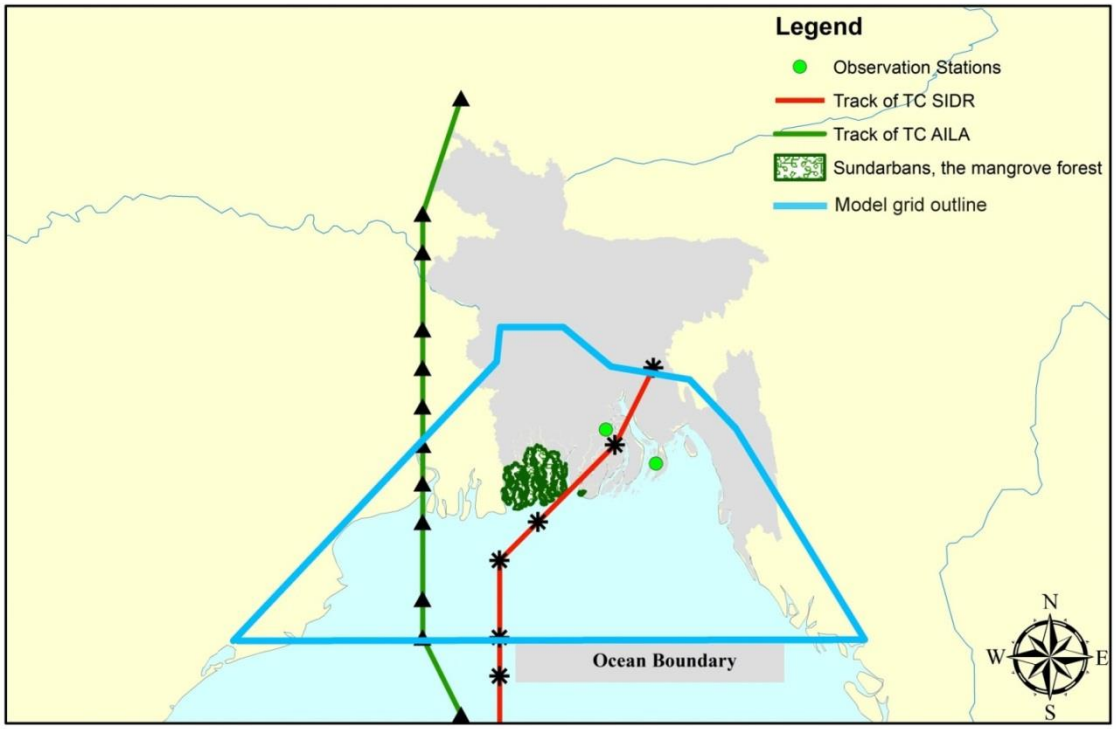

Figure 2: Map of the study area. The red and green lines show the tracks of TC Sidr and TC Aila, respectively. The area marked with green color indicates the Sundarban mangrove forest region. Two green circles over the study area are the observation stations of Bangladesh Inland Water Transport Authority (BIWTA). The blue colored outline shows the extent of Delft3D model grid.

1.1 GOALS AND OBJECTIVES

The goal of this study is to understand how the projected SLR will impact storm surge and inundation area for coastal regions (such as coastal Bangladesh) and those with different coastal land-topographic slopes. To achieve this goal, we will use a well-validated hydrodynamic model to simulate the storm surge and inundation area due to an ensemble of TC tracks for present-day and future SLR scenarios for varying topographical slopes. Our research objectives are thus to:

(1) Use the validated model configuration of Delft3D to quantify the change in simulated storm surge and inundation under the impact of the projected SLR for the Bangladesh coastal region.

(2) Establish the relationship between the topographic slope and the impact of the projected SLR on storm surge and inundation area.

2. METHODOLOGY

2.1 THE DELFT3D-FLOW MODEL

2.1.1 DESCRIPTION OF THE COMPUTATIONAL SUITE

Delft3D-FLOW solves the Navier-Stokes equations for an incompressible fluid, under the shallow water and the Boussinesq assumptions. In the vertical momentum equation, the vertical accelerations are neglected, which leads to the hydrostatic pressure equation. It uses orthogonal curvilinear co-ordinates in the horizontal direction with two supported co-ordinate systems: Cartesian and Spherical co-ordinate. We used the spherical co-ordinate system which is a special case of orthogonal curvilinear co-ordinates. In this thesis Delft3D's 2D mode for barotropic depth-integrated flow has been applied.

This computational suite developed for a multi-disciplinary approach to nearshore wave and morphodynamic modelling. And because of this reason, this modeling suite is composed of several modules which allows user to carry out simulation of flow (Delft3D-FLOW), sediment transport (Delft3D-SED), waves (Delft3D-WAVE), water quality (Delft3D-WAQ) and Delft3D-PART) and ecology (Delft3D-ECO) (Delft Hydraulics, 2006).

In addition to these six modules of this computation suite, Delft3D also includes several programs in order to ease the treatment of raw data. This includes Delft3D-RGFGRID and

Delft3D-QUICKIN. Delft3D-RFGRID allows the generation and modification of orthogonal or curvilinear grids. Therefore, this program is based on a grid generation process that fulfils the Delft3D-FLOW and Delft3D-WAVE requirements of grid smoothness and orthogonality (Delft Hydraulics, 2009).

Major purpose of Delft3D-QUICKIN program is to create, edit and visualize bathymetric data that is an input for the Delft3D-FLOW and Delft3D-WAVE modules. For example, if bathymetric samples (raw data) are added to Delft3D-QUICKIN, a Digital Model of the Terrain may be generated inside a grid domain by using interpolation tools. Also, rapidly-varying bathymetry can be smoothed using a depth smoothing option (Delft Hydraulics, 2006).

Finally, the post processing tool Delft3D-QUICKPLOT can be used to visualize and animate numerical results. Moreover, this program allows a seamlessly integration with the MATLAB environment (Delft Hydraulics, 2009). Delft3D-FLOW manual (Delft Hydraulics, 2009) contains detailed information about these numerical aspects.

2.1.2 GRID

An orthogonal curvilinear staggered grid was created using Delft3D's RGFGRID, a program for the generation and manipulation of curvilinear grids for Delft3D-FLOW. RGFGRID can be used to modify the grid cell's resolution, smoothness and orthogonality (Delft Hydraulics, 2006).

The model grid has been designed such that the area of interest has enough grid cells to represent the accurate bathymetry. The grid-spacing varies from 222 to 1408 meters. The finest grid cells were over the land to specify the depth more accurately from the topographic sample, which is an important factor for simulating inundation properly. Number of grid cells over M-direction was 864 and number of grid cells in N-direction was 1241. In addition to the resolution, some other general guidelines for constructing grids, such as those recommended by Grasmeijer, Adema, & Jellema, (2014), are followed. These guidelines include maintaining the proper aspect ratio, maximum smoothness in both directions, and grid cell orthogonality. Aspect ratio represents the ratio between length and width of a grid cell. Grid cell orthogonality determines the perpendicularity of a cell. Smoothness represents the ratio between the lengths of adjacent grid cells in certain directions. These guidelines are followed in constructing the grid used in the project, and as a result, the maximum orthogonality of the generated grid was 0.67, and the maximum aspect ratio of grid cells was 1.92.

2.1.3 TOPOGRAPHY AND BATHYMETRY

Delft3D's QUICKIN program (Delft Hydraulics, 2009) was used to define the bathymetry of the domain grid. Since high-resolution topography data (i.e. LiDAR) is not available for the Bangladesh region, it is critical to accurately define depths in each of the grid cells, especially given the availability of only relatively coarse resolution data. In this study, the land topography data were obtained from NASA's Shuttle Radar Topography Mission (SRTM) 90-m resolution datasets. The River bathymetry data were collected from the Institute of Water and Flood Management's survey data over the southwestern part of Bangladesh. The ocean bathymetry was defined from the General Bathymetric Chart of the Oceans (GEBCO' 14) 30-arc-sec interval gridded data.

As the data from SRTM and GEBCO are relatively coarse, triangular interpolation and internal diffusion methods from the QUICKIN program were utilized to ensure appropriate generation of depths. The triangular interpolation method is suitable for data sets that have a resolution that is about equal to or lower than the grid resolution. In this method, the samples are first arranged into a so-called Delaunay network, after which grid values are interpolated (Delft Hydraulics, 2009). After conducting the triangular interpolation, missing values at any grid points were processed by the "internal diffusion method" which is a smoothing process that does not change values of existing depth values and thus provides a smooth transition with the existing bathymetry (Delft Hydraulics, 2009).

2.1.4 BOUNDARY CONDITIONS AND PHYSICAL PARAMETERS

Boundary conditions were defined in a time-series format. The upstream river discharge boundary was defined at the mouths of three major rivers: the Ganges, Brahmaputra and Meghna. Daily river discharge data were collected from the Bangladesh Water Development Board. The downstream open ocean boundary was defined at the Bay of Bengal. The time dependent tide data from the TPXO inverse tide model were used as the boundary conditions at the downstream open boundary.

In selecting the Manning's roughness coefficient values, the method described in Zhang *et al.* (2012) was followed and slightly modified based on the vegetation types and land covers. Delft3D's QUICKIN program was used to define these spatially varying roughness values (Table 1). In particular, the southwestern part of the study area is bordered by the Sundarban mangrove forest. According to Sakib *et al.* (2015), Sundarban played a vital role by acting as a buffer against TC Sidr and reduced the impact of Sidr and much of the potential inundation depth and extent of flooding. In this study, we defined a high value of Manning's roughness coefficient for this Sundarban mangrove forest area.

Table 1: Manning's Roughness coefficient for different land cover

Land Cover	**Manning's Coefficient**
River	0.015
Mangrove	0.080
Ocean	0.01
Land	0.025

Among other physical parameters specified in the model, the gravitational acceleration, the densities of water and air, and the horizontal eddy viscosity and diffusivity were prescribed.

2.1.5 WIND AND PRESSURE FIELD

Track data of TCs Sidr and Aila were obtained from the Indian Meteorological Department (www.imd.gov.in). From these tracks, TC surface winds and mean sea level pressure fields were generated using the Wind Enhancement Scheme (WES) (Heming *et al.* 1995) method based on the analytical equation by Holland (1980). Delft3D has slightly improved the original WES by introducing TC asymmetry. Unlike some previous method that incorporates TC wind asymmetry information from observations (Xie *et al.* 2006), in WES the asymmetry is brought about by applying the translation speed of the cyclone center displacement as steering current and by introducing rotation of wind speed due to friction (Heming *et al.* 1995).

According to the Holland's equation, the gradient wind speed $V_g(r)$ at a distance r from the center of the cyclone is expressed as the following:

$$V_g(r) = \left[\frac{AB(p_n - p_c)\exp\left(-\frac{A}{r^B}\right)}{\rho r^B} + \frac{r^2 f^2}{4}\right]^{0.5} - rf/2 \qquad (1)$$

where ρ is the density of air, p_c is the central pressure and p_n is the ambient pressure. The Coriolis parameter is represented by f. The coefficients A and B are determined empirically. The physical meaning of A is the relation of pressure or the wind profile relative to the origin. The parameter B defines the shape of the profile. Delft3D introduces

a central pressure drop of $p_d = p_n - p_c$. By equating $\frac{dV_g}{dr} = 0$, the radius of maximum winds R_w can be given as $R_w = A^{1/B}$

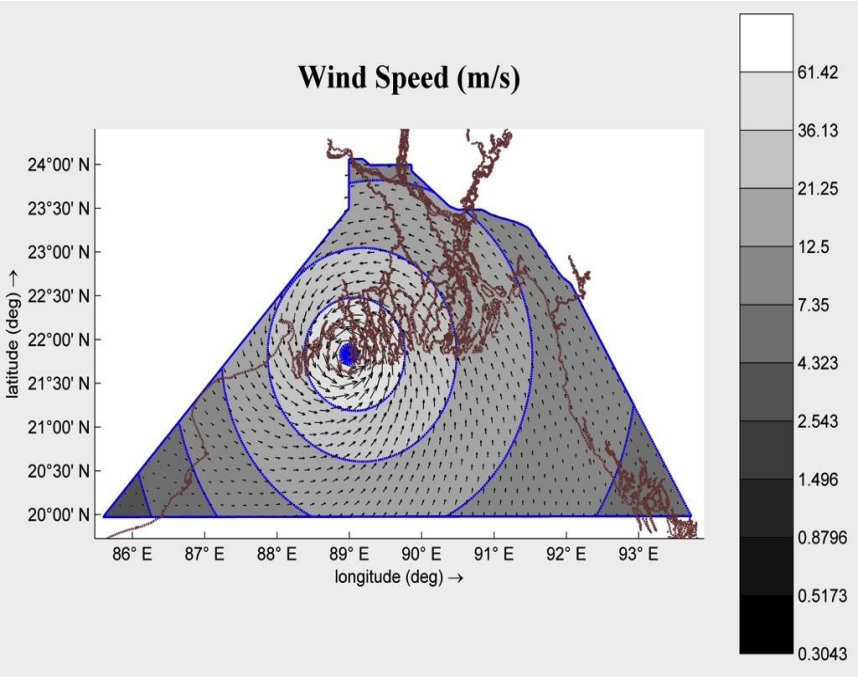

Figure 3: Distribution of the wind speed over the model domain for TC Sidr during its landfall, as generated using Holland's equation.

Thus, R_w is independent of the relative values of ambient and central pressure and is defined entirely by the scaling parameters A and B. Substitutions lead to the expression for the maximum wind speed $V_m = \left[\frac{Bp_d}{\rho e}\right]^{0.5}$

Complete details about this method can be found in the user manual of Delft3D Flow (Delft Hydraulics, 2009), Holland (1980), and Vatvani *et al.* (2002).

The circular grid for TC wind fields used in this study consists of 36 columns and 500 rows, and the data were updated at 6 hourly intervals throughout its movement until landfall

of the eye occurs. Figure 3 shows a snapshot of the wind field of TC Sidr over the model domain, before landfall, generated using Holland's equation described above.

2.2 PRESENT DAY AND FUTURE STORM SURGE AND INUNDATION SCENARIO

To simulate the TC-induced storm surge and inundation in a present-day climate scenario, upstream discharge and downstream water level data from the present were used. For future SLR scenarios, present day upstream discharge and the strength of present-day TCs were used, but the future sea level was modified based on the SLR projections of Caesar *et al.* (2017; under review). SLR scenarios have been generated for both the Mid-21st century and the End-21st century time horizons. To evaluate the impacts of future SLR, comparisons were made between present-day and future SLR scenarios storm surge height and inundation area.

2.3 ENSEMBLE PROJECTIONS OF STORMS SURGE AND INUNDATION

Future TC-induced storm surge and inundation in an SLR scenario have a probabilistic nature whose simulation requires proper addressing of the uncertainties associated with the input TC track and intensity parameters. To address the future TC uncertainties and to obtain statistically significant results, we created an ensemble of TC tracks. The ensemble of tracks consisted of 12 historical TCs that made landfall over the study domain at different locations with varying intensities. Six of the TCs occurred in pre-monsoon (April-May) period and the other six post-monsoon (October-November). Besides the uncertainties associated with future TC tracks and landfall locations, the intensities of future TCs have uncertainty as well. Therefore, to address the uncertainty associated with

future TC intensity, we also varied their intensity by +10% and -10% to simulate the probable range of future storm surge and inundation caused by future TCs.

Storm surge and inundation can also be different based on landfall timing of the TCs that caused them. For example, if a TC made landfall under a high-tide condition, its storm surge level would be higher and inundation area larger than if the landfall during a low tide. TC Sidr and TC Aila both made landfall under high tide conditions, which may not always be applicable for future TCs; however, this is the worst-case scenario. To also address uncertainties associated with the TC landfall timing, we conducted experiments by changing the landfall timings so that they were simulated under both high-tide and low-tide conditions, to identify the impacts of the tidal phases on storm surge and inundation.

Another parameter we considered in the study is the topography of the Bangladesh coast. As mentioned in the Introduction, the present-day flat topography of the Bangladesh coast is one of the major causes behind its vulnerability to TC-induced storm surge and inundation hazards. To investigate this reason numerically and to evaluate the sensitivity of the future SLR's impact on storm surge and inundation to coastal topographic slopes, we conducted ensemble simulation by considering the uncertainties mentioned in Table 2 based on possible future adjusted topographic slope conditions; presently unknown. The actual topographic slope of Bangladesh coast was modified by gradually increasing its rise over the land. In addition to the actual topography, we considered two slope conditions with their slopes being 1.25×10^{-5} and 1.25×10^{-4}, respectively (Figure 4).

In summary, the future TC-induced storm surge and inundation in an SLR scenario were simulated using the ensemble of TC tracks with varying landfall locations, intensities and timing and for different coastal topographic slopes. Accounting for all these parameter

variations, we conducted an ensemble simulation with 324 ensemble members for each present-day and future SLR scenarios. The parameters that were considered in making ensemble projections are shown in Table 2.

Table 2: Parameters considered for the ensemble projection of storm surge and inundation.

TC TRACK	**INTENSITIES**	**TIDE CONDITIONS**	**SLR**	**SLOPE**
TC SIDR	+10%, actual, -10%	high tide, low tide, actual tide, zero tide	Present day, 0.26 m, 0.54 m	actual, moderate, steep
TC AILA	+10%, actual, -10%	high tide, low tide, actual tide, zero tide	Present day, 0.26 m, 0.54 m	actual, moderate, steep
12 HISTORICAL TC TRACKS	actual	actual tide	Present day, 0.26 m, 0.54 m	actual, moderate, steep

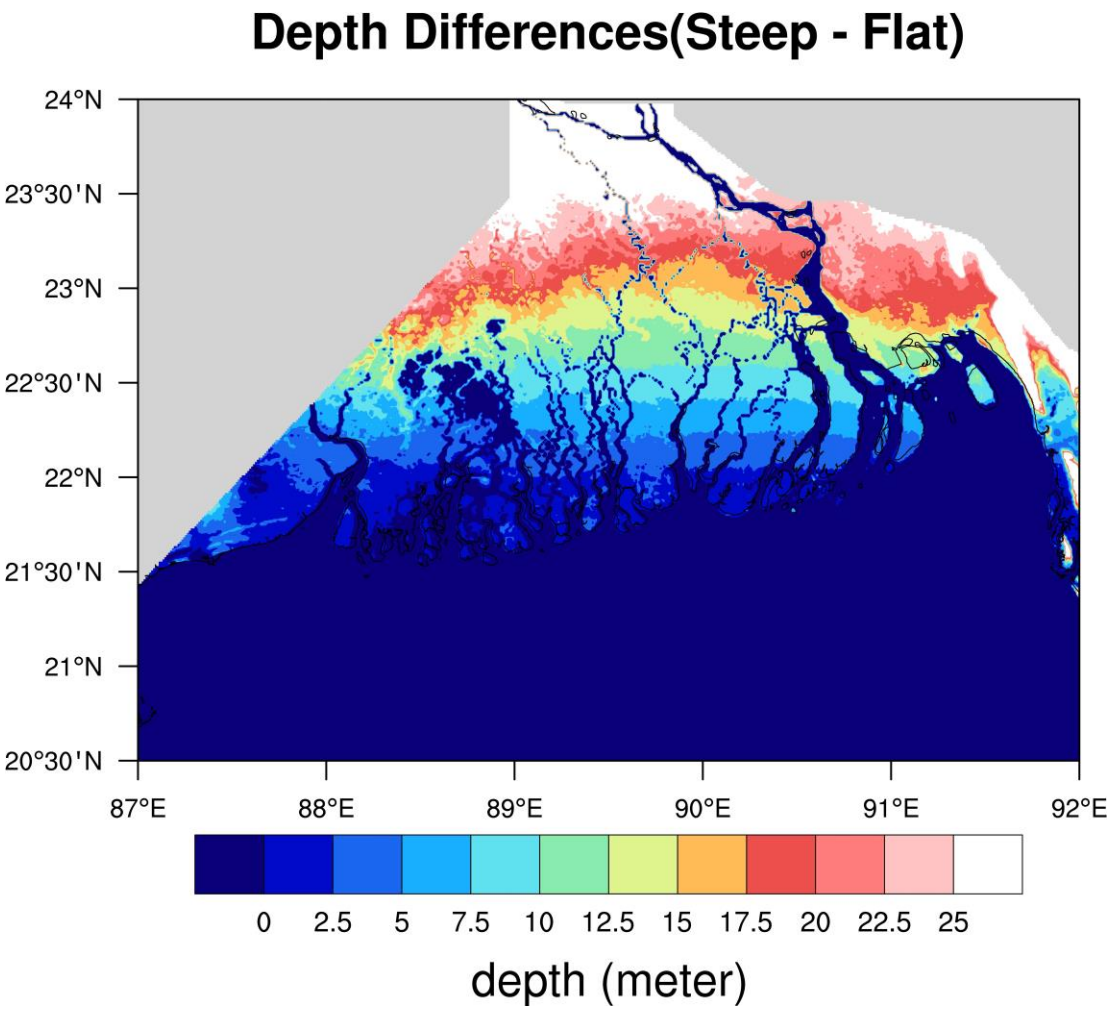

Figure 4: Differences of depths between the flat ($1.25*10^{-5}$) and steep ($1.25*10^{-4}$) topographic slopes considered for the ensemble projections.

3. RESULTS

3.1 VALIDATION OF MODEL RESULT

Hourly tidal data from the Bangladesh Inland Water Transport Authority (BIWTA) were used to evaluate the performance of the model. The model simulation's root mean square error (RMSE) (Equation 2), mean absolute error (MAE) (Equation 3) and dimension-less Nash-Sutcliffe coefficient (E) (Equation 4) (Nash & Sutcliffe 1970) were calculated and listed in Table 3. Nash-Sutcliffe coefficient ranges from negative infinity (-∞, no skill simulation) to one (perfect simulation)

$$\boldsymbol{RMSE} = \sqrt{\frac{\sum_{i=1}^{n}(\boldsymbol{X_{obs,i}} - \boldsymbol{X_{model,i}})^2}{\boldsymbol{n}}} \quad (2)$$

$$MAE = \frac{1}{n}\sum_{i=1}^{n}\left|X_{obs,i} - \hat{X}_{obs}\right| \quad (3)$$

$$E = 1 - \frac{\sum_{i=1}^{n}(X_{obs,i} - X_{model})^2}{\sum_{i=1}^{n}(X_{obs,i} - \overline{X_{obs}})^2} \quad (4)$$

Table 3: RMSE, MAE and Nash-Sutcliffe coefficient for the storm surge level model validation for TCs Sidr and Aila

	TC Sidr			TC Aila		
	RMSE (m)	MAE (m)	NASH	RMSE (m)	MAE (m)	NASH
Barisal	0.23	0.16	0.85	0.33	0.24	0.65
Charchanga	0.26	0.19	0.80	0.28	0.17	0.73
Average	**0.245**	**0.175**	**0.825**	**0.305**	**0.205**	**0.69**

The locations of the two observation stations were not ideal for model validation purpose. The Barisal station is located farther inland whereas Charchanga is located near the coastline where the grid cell resolution was coarse. None of them are in the open ocean water, which is important to get a clear idea about the level of the storm surge. Additionally, TC Aila made landfall far from these two observation stations, and therefore its impact was not as clear as that of TC Sidr, whose landfall location was close to the two stations. Nevertheless, due to the lack of higher quality observational data, the simulated water levels were compared against the measured data at Barisal and Charchanga (Figure 2).

In Figure 5(a) for TC Sidr at the Barisal station, the modeled water level, including storm surge and astronomical tides, was slightly lower than the observations, especially after the passage of the TC. At the Charchanga station (Figure 5b) the measured water level variation displayed larger amplitudes than did the model output, and the modeled water level was higher than the observed one. Similar types of variations between measured and modeled water level was found also for TC Aila (Figures 5c and 5d). These discrepancies are likely due to the inaccurate bathymetry. Nevertheless, the modeled water level

variations during TCs Sidr and Aila agreed reasonably well with measured data, as also confirmed by the average RMSE, MAE and Nash-Sutcliffe coefficient. Therefore, we concluded that the model configuration can be used to study the impact of SLR on storm surge and inundation in future climate change scenarios.

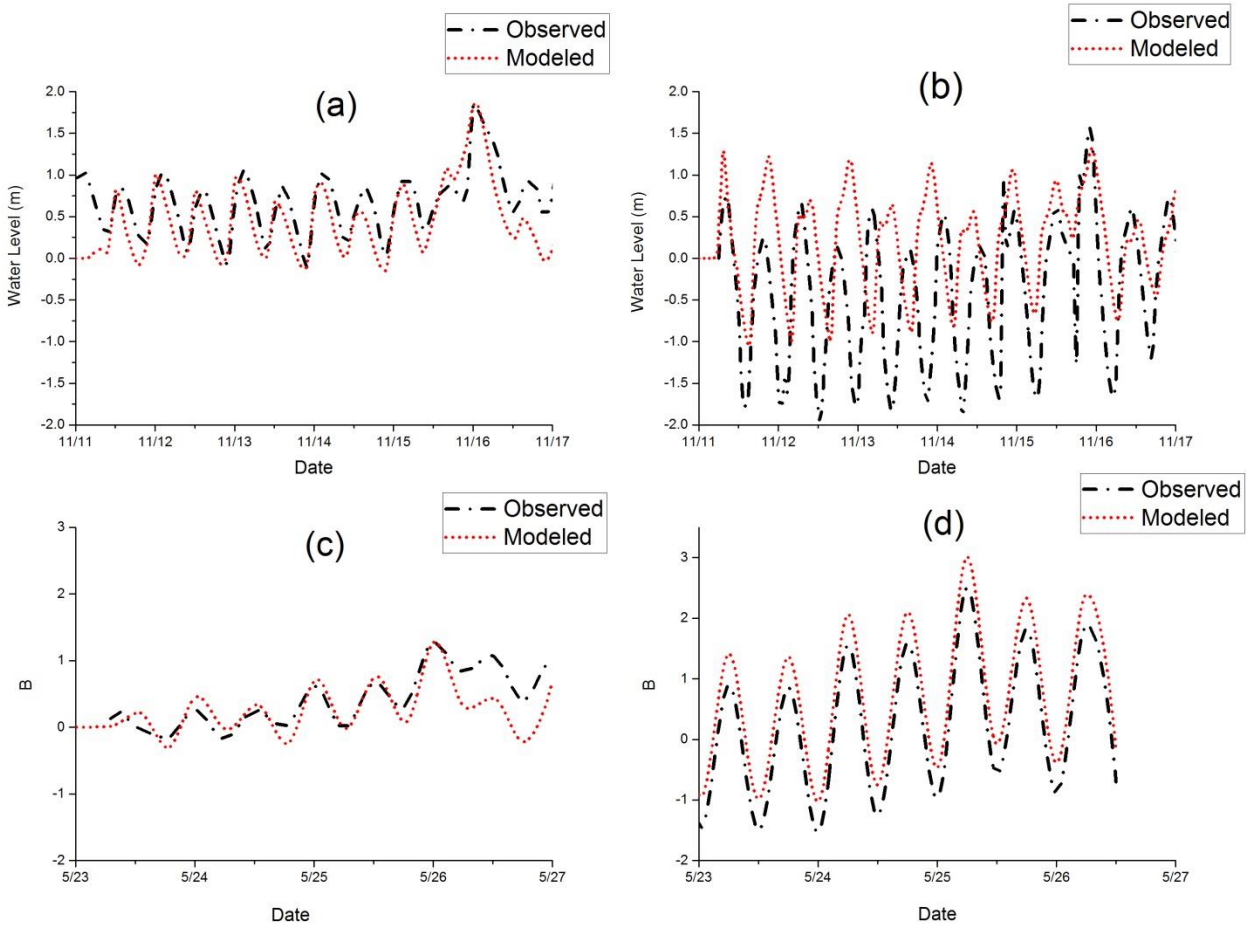

Figure 5: Comparison of the observed and modeled water level (a) for TC Sidr at Barisal (b) for TC Sidr at Charchanga (c) for TC Aila at Barisal (d) for TC Aila at Charchanga.

3.2 PRESENT DAY INUNDATION SCENARIO

The simulated present-day inundation scenarios caused by TCs Sidr and Aila are shown in Figure 6. The inundation area caused by TC Sidr (yellow shade+red shade) was much higher than that caused by TC Aila (white shade+red shade), a result that is consistent with the fact that the TC Sidr (category-5) was much stronger than TC Aila (category-1) and also directly hit the study area. The maximum sustained wind speed of TC Sidr was 72 m s^{-1} whereas for TC Aila it was 30 m s^{-1}. The landfall location of Sidr was on the eastern side of Sundarban, while Aila's landfall location was towards the western side of Sundarban. That explains why the inundation areas due to TC Sidr were located near the eastern side of Sundarban, whereas for Aila, the inundation was located mainly in the western part. The extent of inundation due to Sidr (1860 km^2) was 35% larger than that of Aila (1208 km^2).

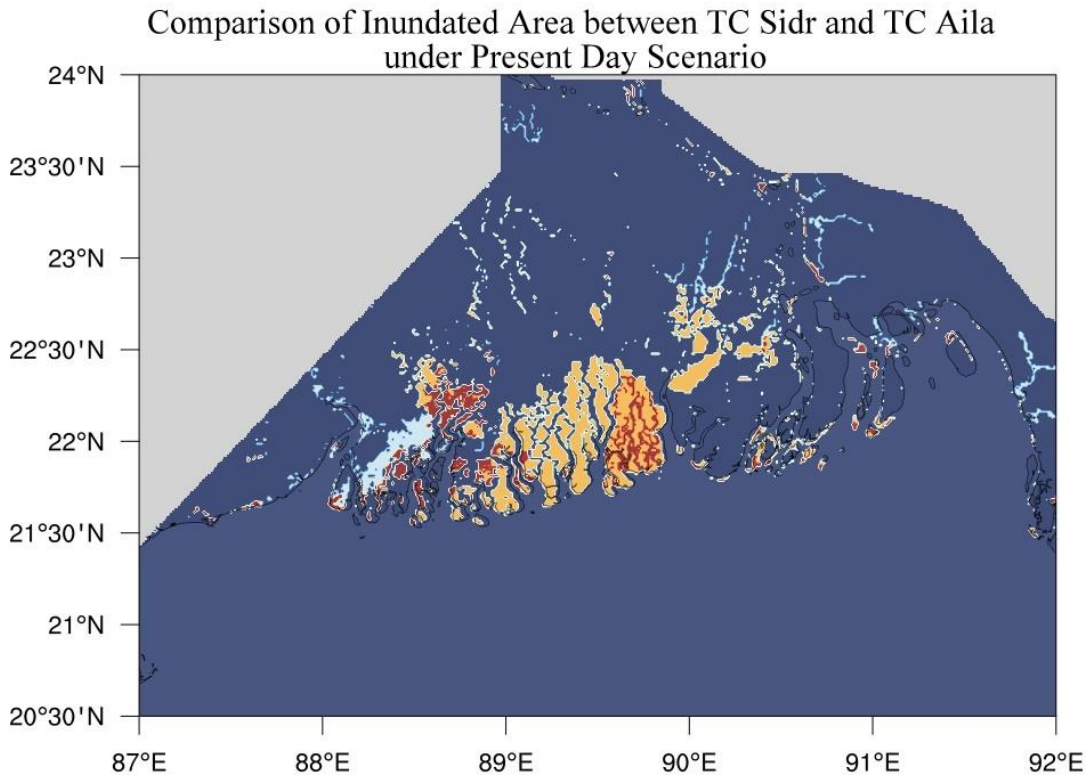

Figure 6: A yellow colors denotes the areas flooded by TC Sidr but not in Aila, and the white color representing the area inundated by TC Aila but not in Sidr. Red color is the area flooded by both TC Sidr and TC Aila. Blue color is showing the non-flooded area (either land or constant water).

3.3 IMPACT OF PROJECTED FUTURE SLR ON STORM SURGE AND INUNDATION CAUSED BY TCS SIDR AND AILA

In this section we seek to answer the question: if TCs Sidr and Aila were to happen under the projected future SLR scenarios, what storm surge and inundation hazards would they cause? Therefore, the tracks and intensities of TCs, Sidr and Aila were used as the model wind input. In next section, this method will be extended to an ensemble of TC tracks and intensities, landfall timings and coastal terrain slopes, to address the uncertainties associated with future TCs and coastal terrain variations.

Future inundation scenarios were generated for two different time horizons: one for the mid-21st century and the other for the end of the 21st century. The initial ocean water level, including the downstream ocean boundary condition, was raised by 0.26 meters and 0.54 meters for the mid-21st century and end-21st century, respectively. The upstream river discharge remained the same as that used in the present-day climate scenarios.

Figure 7 shows that under future SLR scenarios, the inundated areas caused by TCs Sidr and Aila would be significantly higher than those under the present-day climate condition, as indicated by the white color shaded areas. For the category-5 TC Sidr, the inundated area would be 31% and 53% higher than present day's 1860 km^2 inundated area, in the mid-21st century (0.26 meter SLR) and end of-21st century (0.54 meter SLR) climate scenarios, respectively (Figure 7a, 7b). Similarly, for the category-1 TC Aila, there would also be an increase in inundated area. The simulated inundated areas for TC Aila under the mid-21st century and end-of-21st century were 1550 km^2 and 1770 km^2, respectively (Figures 7c and 7d) ,whereas for the present-day scenario it was found to be 1208 km^2.

All these simulations have been carried out using the present-day tides, upstream river discharges and TC tracks and strengths, with only the initial sea water level raised to reflect the effect of the projected future SLR. Therefore, the results suggest that even if the future TCs strengths, tides and river discharges remain the same as in the present-day climate condition, future SLR would significantly increase the inundated area, by as high as 53%

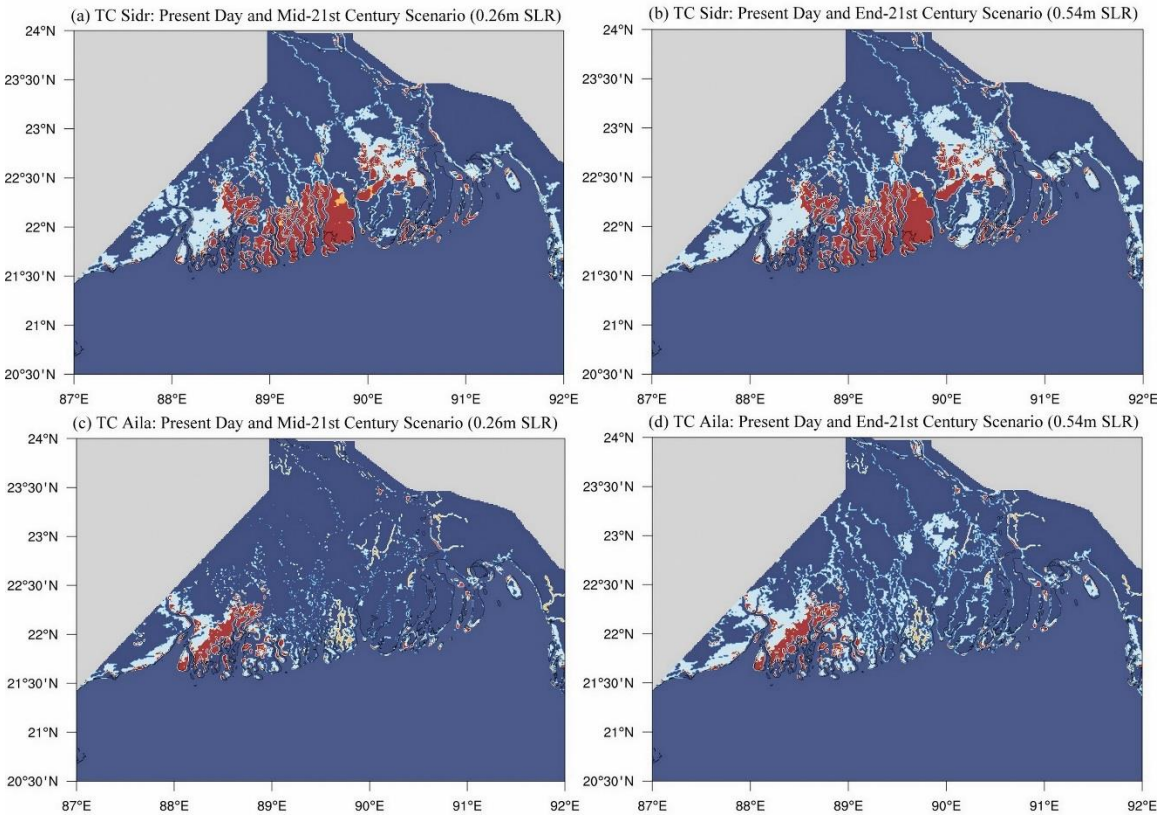

Figure 7: Comparison of inundated area between present day and future climate scenarios for (a) TC Sidr mid-21st century 0.26 m SLR (b) TC Sidr end-21st century 0.54 m SLR (c) TC Aila mid-21st century 0.26 SLR (d) TC Aila end-21st century 0.54m SLR. White color is representing the increased flooded areas that were not in present day scenario but the increase due to future SLR. Red color is showing the inundated areas that are similar both for present day and future scenario case. Blue areas are non-flooded areas. Yellow color is showing the areas that were part of present day inundation but was not flooded during the future SLR conditions.

In addition to the inundation area, the projected future SLR would also significantly affect storm surge levels. Like the approach used in the inundation study, TCs Sidr- and Aila-induced storm surges in the projected future SLR scenarios were simulated.

The simulated storm surge water levels in the future SLR scenarios have been compared with both the observed and model generated ones under the present-day scenario (Figure 8).

For TC Sidr, the simulated peak storm surge level under the mid-of-21st century SLR scenario would be 2.3 m at the Barisal station, around 21% higher than that in the present-day scenario (Figure 8a.). It is to be noted that, there's a slight shift in phase occurred during the period of November 13 to November 15. This could happen due to the presence of seiche. However, for rest of the period, phase variations are similar to the observed one. Similarly, under the end-of-21st century 0.54 meter SLR scenario, the peak storm surge level at the Barisal station would reach 2.6 m, 37% higher (Figure 8a.) than that in the present-day scenario. Similar impacts of the projected SLR on the storm surge level have also been found at the Charchanga station and for TC Sidr. For TC Sidr at the Charchanga station, the simulated peak storm surge levels would be 2.24m in the mid-of-21st century (0.26 m SLR) scenario and 2.59 m in the end-of-21st century (0.54 m SLR) scenario, 14% and 31% higher than that in the present-day scenario, respectively (Figure 8b). For TC Aila at Barisal, the simulated peak storm surge levels would be 1.61m in the mid-of-21st century scenario and 1.96 m in the end-of-21st century scenario, 22% and 51% higher than that in the present-day scenario, respectively (Figure 8c). For TC Aila at Charchanga, the simulated peak storm surge levels would be 3.01m in the mid-of-21st century scenario and 3.37 m in the end-of-21st century scenario, 50% and 68% higher than that in the present-day scenario, respectively (Figure 8d).

It should be noted that the present-day datum is used to calculate the storm surge water levels in the projected SLR scenarios. Therefore, the increase in the simulated storm surge water levels in the projected SLR scenarios can be attributed largely to the increase in the baseline initial ocean water level. Other than that, the simulated relative water level

changes in the SLR scenarios should be similar to those in the present-day, as suggested by simplified storm surge height equation described in Introduction.

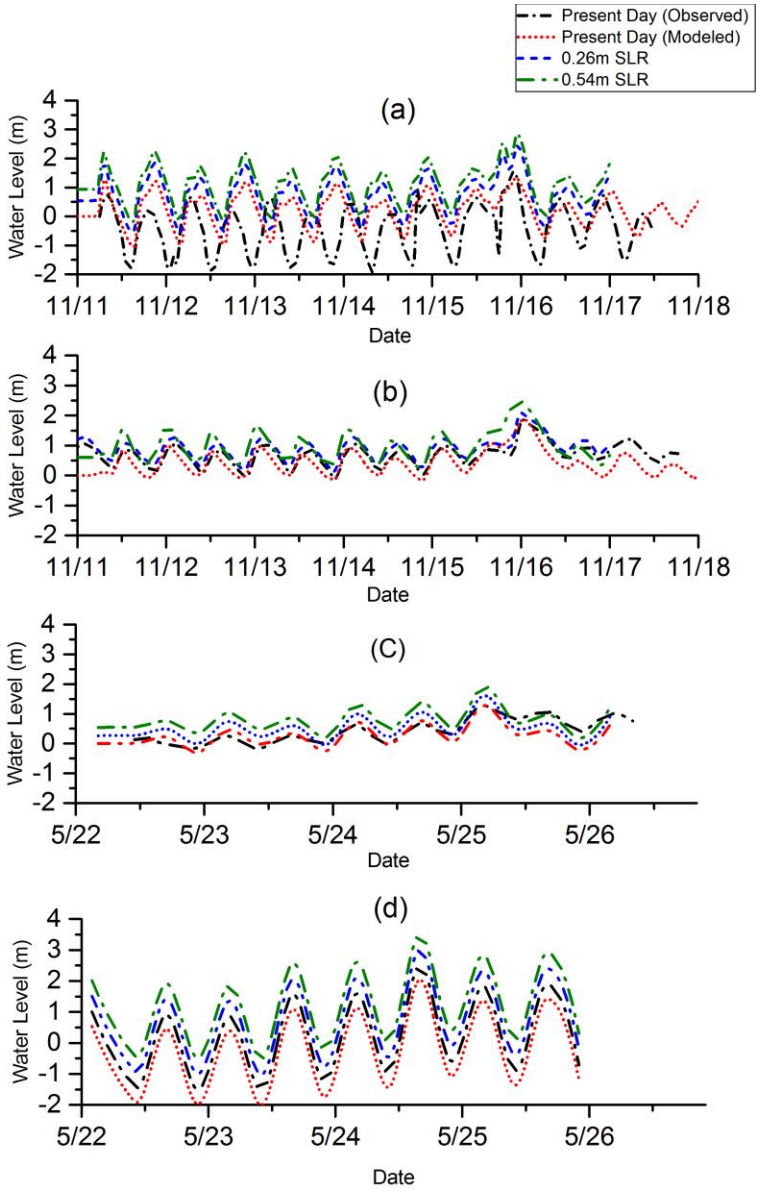

Figure 8: Comparison of storm surge water level (a) TC Sidr at Barisal (b) TC Sidr at Charchanga (c) TC Aila at Barisal (d) TC Aila at Charchanga. The observed, modeled present-day, mid-of-21st century and end-of-21st century storm surge levels are denoted by the solid, red dashed, blue dotted, and red dash-dottted lines, respectively.

3.4 ENSEMBLE PROJECTION OF FUTURE STORM SURGE INUNDATION UNDER SLR CONDITIONS

In the previous section, results of deterministic simulations showed that the projected future SLR would significantly increase the storm surge water level and inundation areas caused by TC Sidr and Alia. However, there are large uncertainties in the intensities, landfall locations and timings of future TCs. As discussed in Section 2.3, to address these uncertainties, an ensemble of probable future TCs was constructed by considering all the uncertainty factors mentioned in Table 2, and the 324 ensemble members were used to simulate the storm surge and inundation in the two projected future SLR scenarios. Results of the simulations using the 108 ensemble members with the actual coast topographic slope showed evidence for increases in the inundation area under the effect of projected future SLR (Figure 9). Of the 36 present-day scenario simulations (black column), the peak column, i.e., the number of simulations of which the inundation area would likely occur between the range of 1000-1250 km^2, is 13. For the simulations in the projected 0.26 m SLR scenario, the peak column shifted towards the right side, and the maximum frequency of inundation events, 10 out of the 36 simulations, caused inundation areas within the range of 2000-2250 km^2. For the simulations in the projected 0.54 m SLR scenario, the peak column shifted further towards the right side, and the maximum frequency of simulations, 11 out of 36, showed inundation areas in the range of 3500-3750 km^2. These results show that the increase in inundation areas under the projected SLR scenarios is not limited to TCs Sidr and Alia. Instead, that simulated impact of the future SLR on inundation area has general significance and robustness, and is valid even when the uncertainties associated with future TCs, such as their tracks, intensities and landfall timings, are considered.

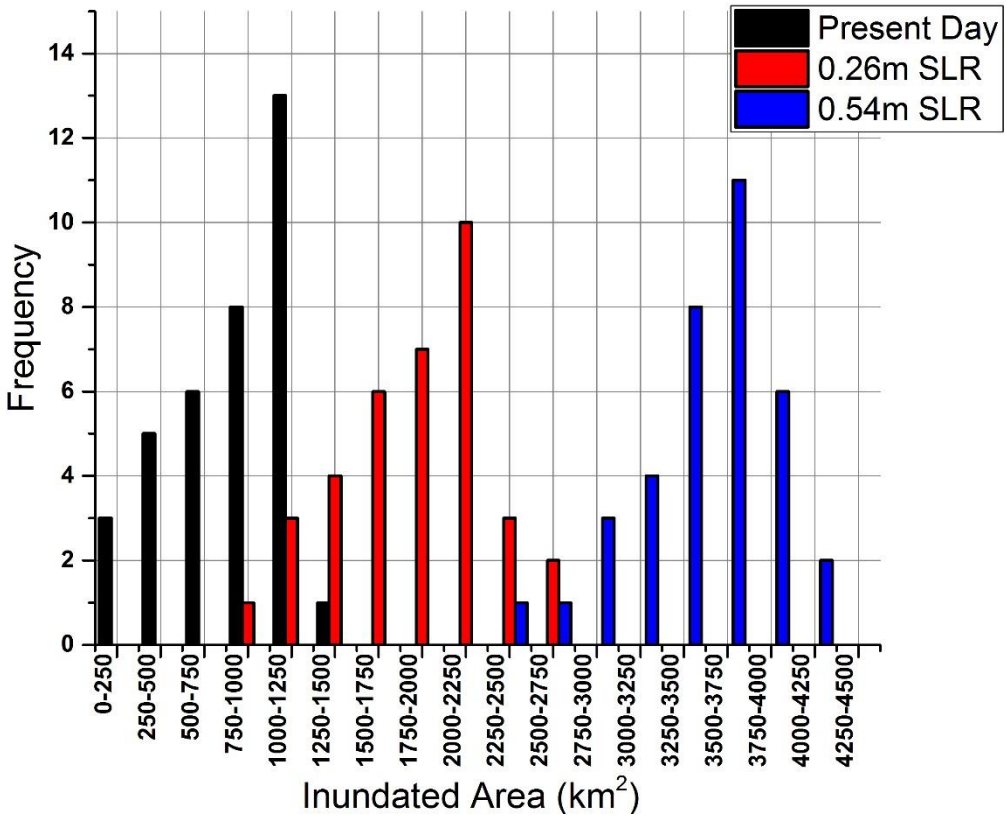

Figure 9: The relation of the number of storm surge and inundation simulations and the simulated inundation area, in the present-day and the two projected SLR scenarios. area. The columns in black color are representing the events for the present day sea level condition, red colored ones are for 0.26 m SLR and blue colored columns are for 0.54 m SLR scenarios. In total, 108 simulations were conducted.

3.6 RELATION BETWEEN TOPOGRAPHIC SLOPE AND INUNDATION AREA UNDER SLR SCENARIOS

A steep and a relatively flat topographic slope could conceivably affect the inundation area in a significant way. To evaluate this effect numerically, we conducted a 108-member ensemble simulation for each of two different topographic slope conditions. In each of these two ensemble simulations, the model configuration was the same as that used in Section 3.5, except that the topography data was modified to have a different slope. The two modified topographic slopes included a steep one of $1.25 \text{ X } 10^{-4}$ and a moderately steep one of $1.25 \text{ X } 10^{-5}$.

The ensemble simulation result with the steep topography is shown in Figure 10. Under the present-day sea level scenario, the highest frequency of events, 20 out of 36, caused an inundation area within the range of 500-750 km^2. Under the 0.26 m SLR condition, the inundated area was increased, and the highest frequency of simulations, 16 out of 36, showed an inundated area in the range of 1000-1250 km^2. Under the 0.54 m SLR condition, the range of inundation was increased even more, and most of the simulated inundated areas, 19 out of 36, fell within the range of 1250-1500 km^2.

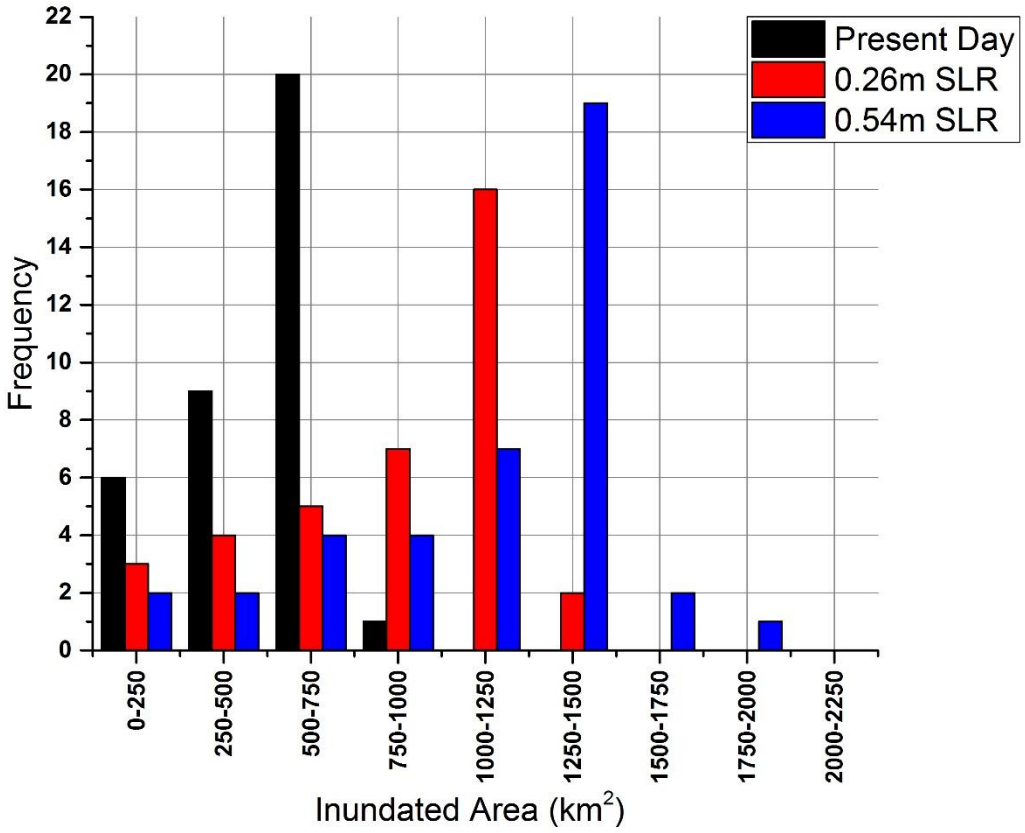

Figure 10: The relation of the number of storm surge and inundation simulations and the simulated inundation area for the moderately steep topographic slope (1.25x10-5), in the present-day and the two projected SLR scenarios. area. The columns in black color are representing the events for the present day sea level condition, red colored ones are for 0.26 m SLR and blue colored columns are for 0.54 m SLR scenarios. In total, 108 simulations were conducted.

Under the 1.25 x 10^{-5} moderately steep slope condition, another 108-member ensemble simulation was conducted. Out of the 36 simulations for the present day sea level condition, 17 showed the range of inundated area within 750-1000 km^2. Under the 0.26 m SLR scenario, the highest frequency events, 13 out of 36, showed the inundation area in the range of 1250-1500 km^2. Under the projected end-of-21st century 0.54 m SLR scenario, the highest frequency events, 17 out of 36, caused an inundation area within the range of 1750-2000 km^2 (Figure 11).

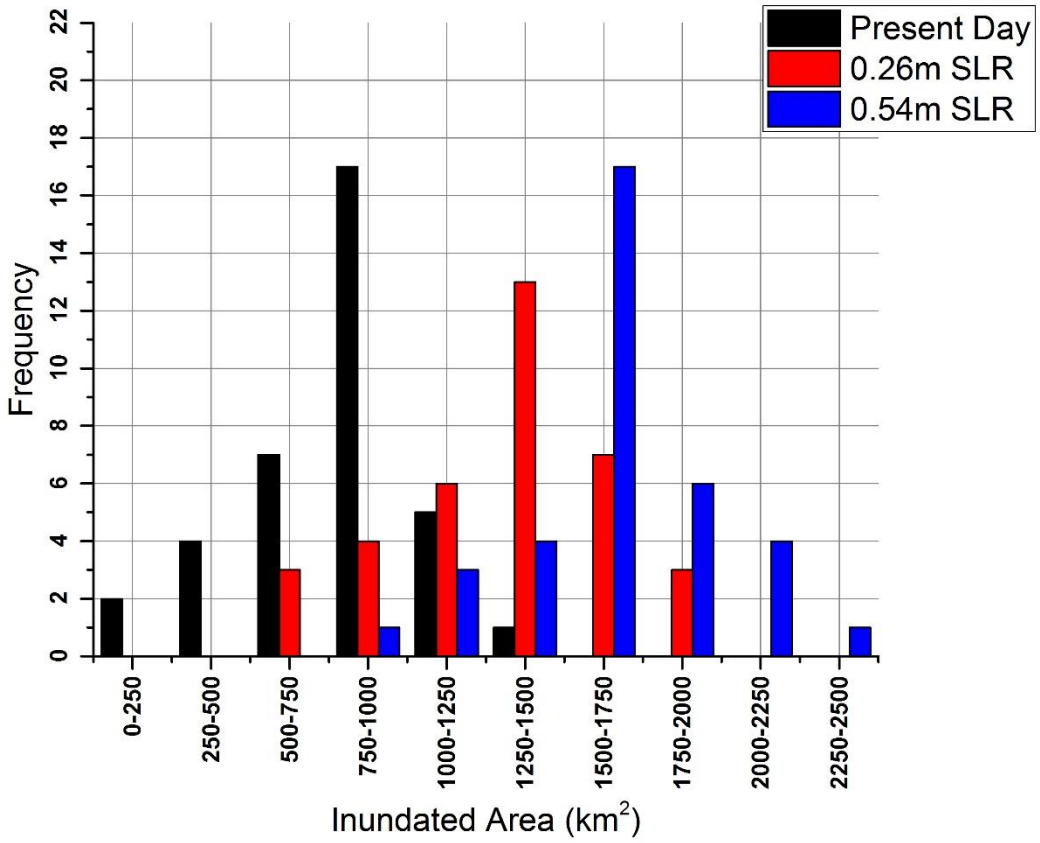

Figure 11: The relation of the number of storm surge and inundation simulations and the simulated inundation area for the moderately steep topographic slope (1.25x10-5), in the present-day and the two projected SLR scenarios. area. The columns in black color are representing the events for the present day sea level condition, red colored ones are for 0.26 m SLR and blue colored columns are for 0.54 m SLR scenarios. In total, 108 simulations were conducted.

If we analyze the inundated area distributions simulated under these two modified topographic slope conditions and compare them with the simulated inundation area under the actual topography condition, we found that due to the actual flat topography of coastal Bangladesh, the inundation area was larger when the actual topography was used. For example, under the condition of actual slope and present-day sea level condition, the most probable range of inundated area was 1000-1250 km^2 (Figure 9), while under the steep topography condition, the most probable inundation area fell in the range of only 500-750

km^2 (Figure 10). These results yield insights into how the inundated area can be different based on the characteristics of the topographic slope.

Figure 12 shows the most probable inundation areas in the ensemble simulations and their relations with the projected future SLR scenarios and coastal topographic slopes. In plotting these lines, we used the mid-point values of the highest frequency (thus most probable) ranges of the inundation area. For example, under the actual topographic slope condition of Bangladesh, the most probable range of inundation was 1000-1250 km^2 (Figure 9) for the present day sea level condition; as such, the mid-point value of this range, 1125 km^2, was plotted in Figure 12. A similar approach was taken for the two additional future projected SLR conditions. We again selected the mid-point values from the most frequent events of inundation for moderately steep ($1.25x10^{-5}$) and very steep ($1.25x10^{-4}$) topographic slope conditions.

From Figure 12 one can see that even if the slope steepens, the inundated area still increases because of SLR. However, the rate of increase is not as high for a steep slope as it was found for the present day actual flat topographic slope of Bangladesh. Under the present-day sea level condition, the inundated area decreases gradually as the topographic slope increases. The most probable inundated area of 1125 km^2 under the present day actual topography of Bangladesh, changed to 875 km^2 and 625 km^2 respectively as the slope became moderately steep and very steep relative to today's actual slope. A similar trend can be seen for the 0.26 m and 0.54 m SLR conditions in that their most probable inundated area also decreased with the increasing slopes. For all three topographic slopes, the most probable inundated area increased with the projected SLR. For example, under the 0.26 m and 0.54 m cases of SLR, with the present day actual topographic slope of Bangladesh, the

most probable inundated area became 2125 km^2 and 3625 km^2 respectively whereas in the present-day sea level scenario it was only 1125 km^2. As we made the slope moderately steep, the most probable inundated area on the present-day sea level scenario decreased to 875 km^2 for the present day sea level condition, but the most probable inundated areas were 1375 km^2 and 1625 km^2 respectively due to 0.26 m and 0.54 m of SLR. Similar trends can be observed for very steep slope condition.

In summary, according to the 324-member ensemble simulation, the most probable inundated area always increased with the projected future SLR and decreased with the rising topographic slopes. However, the impact of the projected SLR on the most probable inundated area was most significant when the present-day actual flat topography was used, as the most probable inundated area increased by 2500 km^2 due to the projected 0.54m SLR. When the topographic slopes were increased, the impact of the SLR on the inundated area became less than that with the flat topography, and only increased by 750 km^2 due to the same projected 0.54 m SLR.

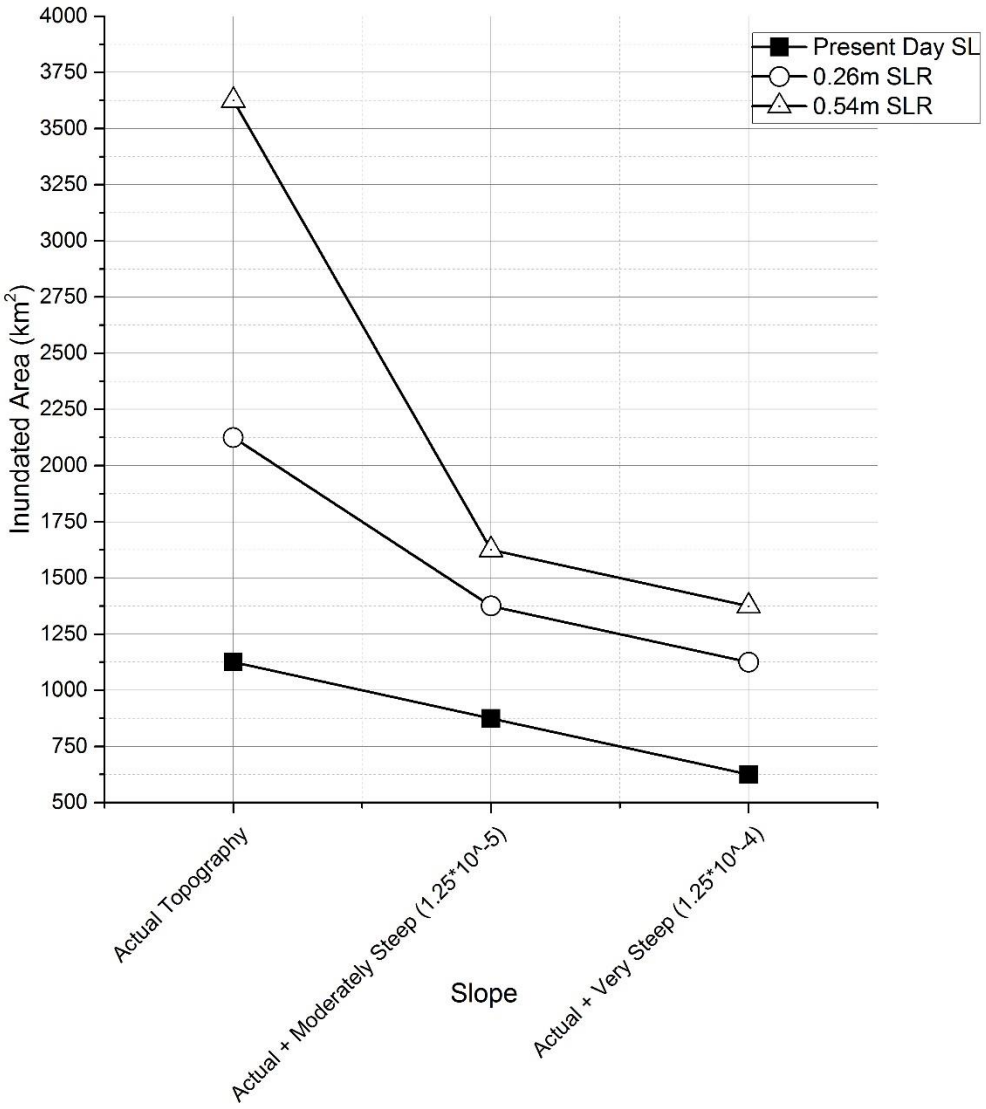

Figure 12: Comparison of inundated area under different topographic slope conditions and for present day & 0.26m and 0.54m of SLR. Line with filled color box is representing the inundated area for present day SL conditions. Line with void circulars representing the inundated area for 0.26 meter SLR and line with void triangular shapes representing inundated area under 0.54 meter SLR.

4. DISCUSSIONS

The model results showed that even if future TCs remain the same strength like the present day ones or increase or decrease slightly (by 10%) and made landfall either in high tide or low tide conditions, their impact will be much higher in a changing climate due to the effect of SLR. Several other factors not included in the modeling could make the storm surge and inundation situation far worse than what is shown in the modeling result. These factors include mangrove coverage decrease in future scenarios, morphological changes, TC strength increase, and upstream river discharge changes.

In including the effect of future SLR in the model simulations, several methodologies were examined. One of the methods experimented in this study is to include the increased sea level in open ocean boundary instead of adding it into the whole ocean depth by keeping the coastline fixed. In such case, an additional pressure gradient force was found acting towards the coast which made the inundated area much higher.

To make the future SLR simulation realistic, we considered the increased sea level in ocean topography and increased the depth by 0.26 and 0.54 m, respectively, by considering land submergence near the coast. In that case, the result looked much realistic than the previous one and this is the employed method. For example, for the case of TC Aila under the end-of-21st century scenario where we used an SLR of 0.54 m SLR at the open ocean boundary instead of adding it to ocean depth and using the hydrodynamic conditions from the present day, the total inundated area has been found to be 79% higher than the present day one.

Similar to that, for the mid-21st century scenario (a 0.26 m SLR), the inundated area has been found to be 69% more than the present-day scenario. But when we added the SLR in ocean depth, the mid-21st-century and end-of 21st century inundated areas have been found to be 28% and 46% higher than the present-day scenario, respectively. This increase in inundated area is much less than the one that we found by adding the SLR in the open ocean boundary. Figure 13 displays the differences in inundated area based on the consideration of SLR in the model input.

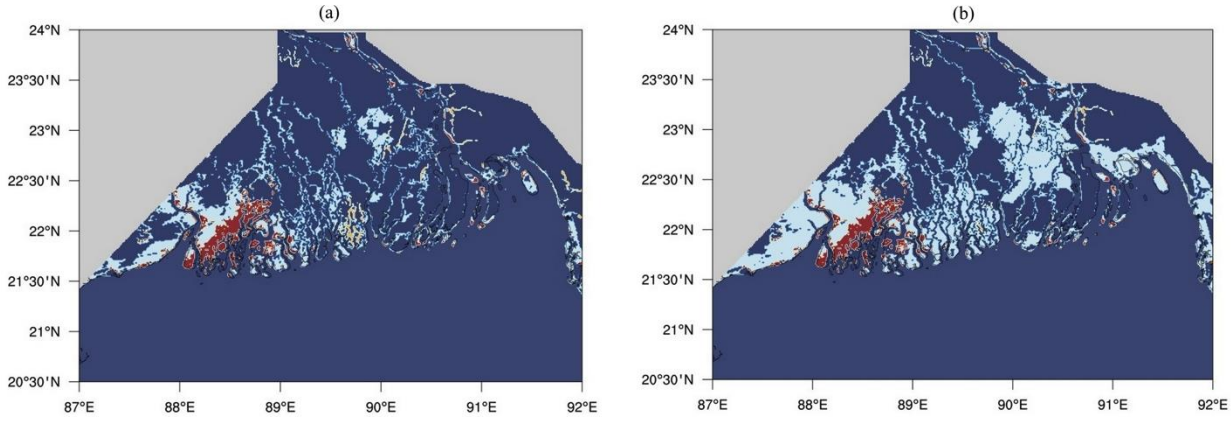

Figure 13: Comparison of inundated areas for TC Aila between present day and end-21st century (0.54m SLR) scenario. White color is representing the increased flooded areas that were not in present day scenario but the increase due to future SLR. Red color is showing the inundated area that's similar both for present day and future scenario case. Blue areas are either land or constant waters (those which are already water at the model initialization time). Figure (a) is representing the inundated area when considered the SLR on ocean depths instead of adding it in to the open ocean boundary and figure (b) showing the inundated area when we considered the SLR on ocean boundary

As discussed, TC Sidr made landfall near Sundarban, where the mangrove forest zone acted as a buffer in reducing the impact of the storm surge flood. That is why, even though a category 5, TC Sidr's impact was not as high as it might have been expected. In this study, the roughness of the mangrove forest zone on the South-West part of Bangladesh was considered to be fixed for the present day as well as for future scenarios. Mukhopadhyay

et al. (2015) predicted that 17% of the total mangrove cover could disappear by 2105. If this decreasing trend of vegetation were considered in this study, the flooded area could be much higher.

Morphological changes were not considered in this study. According to Goodbred et al. (2003), each year the eastern, central and western estuaries are losing land at a rate of 0.13 cm $year^{-1}$, 0.16 cm $year^{-1}$ and 0.16 cm $year^{-1}$, respectively. This could also lead to increased inundated areas for future scenarios. However, as the focus of the paper is to predict the future scenario of storm surge and inundation due to the effect of SLR and comparisons with respect to the present day scenarios, it is important that we keep the roughness and morphological changes constant so that consistent comparisons can be made.

Outputs from the slope-inundation relation under changed sea level showed that even coasts with steep topographic slope will face the consequences of increased sea level. Model results showed that the rate of change in storm surge inundated area under SLR conditions would be higher for countries with a flat topographic slope (i.e. Bangladesh) comparing it with steep topographic slope regions. But both these types of topographic slopes will face an increase in storm surge and inundation under future SLR conditions

Some previous research showed that there could be increases in hurricane strength and landfall probability in the future due to global climate change. Though we slightly modified the present-day TC strengths and selected 12 historical TC tracks to reduce landfall uncertainties and to make ensemble projection of future storm surge inundation, strength may be much higher than the ones we considered in this study. In such cases, the

devastation could be much higher under the projected SLR conditions; which is very alarming.

In this thesis, we used the present-day river discharge data as an upstream boundary for generating future inundation scenarios. But using the INCA-N, an Inland Catchment Modeling system and considering projected climatic & socio-economic scenarios, Whitehead et al. (2015) showed that, there will be a significant increase in future monsoon intensities due to the impact of climate change. That would make future flooding scenarios much worse than those experienced presently. So, based on the changes in TC intensity, river discharges and land-use changes, the situation could well become more badly impacted than what we found in this study.

The findings of this thesis are important for local governments to consider while they make new management and policy decisions and to improve TC preparedness plans by increasing numbers of shelters and heights. Generally, in TC shelters, the first floor is kept transparent due to the risk of high surge waters. Our study showed that, in the future, there will be an increase in surge level from a minimum of 15% up to 70% if a TC of category 1 or 5 makes landfall under increased SLR conditions. So, the authority may consider increasing the height of the first floors for the safety of local populations considering the future risk of the increase in storm surge level and inundation area. Also, our model outputs showed that the inundated area increase would range from 28%-53% percent if a TC of category 1 or 5 were to make landfall with a projected SLR of 0.26 m or 0.54 m. This shows that a huge number of new areas are going to face the impacts of storm surge and inundation. Considering this issue, it is high time to increase the number of TC shelters in the coastal areas of Bangladesh.

5. CONCLUSION

Employing the Delft3D-FLOW model, we simulated coastal storm surge and inundation for present day and future SLR scenarios and compared their relative changes. After validating the present day model, simulations were conducted for the mid-of-21st-century and end-of-21st-century climate scenarios where the SLR has been projected to be 0.26 m and 0.54 m respectively. Model results show that, with an SLR of 0.26 m and 0.54 m, there would be an increase of 38% and 48% of inundated area respectively if TC Sidr were to made landfall with its present day path and strength. For the Category-1 TC Alia, the increase of inundated area would be 25% and 34%. Outputs from the ensemble projections showed that even if the TC intensities, landfall location and timings are uncertain, the most probable range of the TC-induced inundated are would shift from 1000-1250 km^2 (present day) to 2000-2250 km^2 (0.26 meter SLR) and 3500-3750 km^2 (0.54 meter SLR). Besides the inundated area, we also found that storm surge levels would also increase if TC Sidr and TC Aila would make landfall under the projected future SLR conditions. The experiments using topography data with different slopes showed that the projected future SLR would cause the storm surge level and inundation area to increase regardless of the steepness of the topography. However, the impact of the projected SLR on the most probable inundated area was most significant when the present-day actual flat topography was used. When the topographic slopes were increased, the impact of the SLR on the inundated area became less than that with the flat topography. The significant increase in

simulated storm surge and inundation hazards highlights the need for the local governments to improve cyclone preparedness in future SLR scenarios.

REFERENCES

Ahmed R, Falk G C 2008. Bangladesh - Environment under Pressure, In: Geographische Rundschau International Edition, Vol. 4, pp 12-20.

Ali, A., 1996. Vulnerability of Bangladesh to climate change and sea level rise through tropical cyclones and storm surges, in: Climate Change Vulnerability and Adaptation in Asia and the Pacific. Springer, pp. 171–179.

Alam, M., 1996. Subsidence of the Ganges—Brahmaputra delta of Bangladesh and associated drainage, sedimentation and salinity problems, in: Sea-Level Rise and Coastal Subsidence. Springer, pp. 169–192.

BODC, 2003. Centenary Edition of the GEBCO Digital Atlas, published on CD-ROM on behalf of the Intergovernmental Oceanographic Commission and the International Hydrographic Organization as part of the General Bathymetric Chart of the Oceans. British oceanographic data centre, Liverpool.

Caesar, J., Janes, T.,Lindsay, A. 2017. Climate projections over Bangladesh and the upstream Ganges-Brahmaputra-Meghna system, under review, Environmental Science: Processes & Impacts (Under Review).

Chowdhury A M R, Bhuyia A U, Choudhury A Y, Sen R 1993. The Bangladesh cyclone of 1991: why so many people died. Disasters 17, 291 304.

Chowdhury KMMH 2002. Cyclone preparedness and management in Bangladesh: BPATC Improvement of early warning system and responses in Bangladesh towards total disaster risk management approach, BPATC, Savar, Dhaka, pp 115 119

Egbert, G.D., Bennett, A.F., Foreman, M.G., 1994. TOPEX/POSEIDON tides estimated using a global inverse model.

Goodbred, S.L., Kuehl, S.A., Steckler, M.S., Sarker, M.H., 2003. Controls on facies distribution and stratigraphic preservation in the Ganges–Brahmaputra delta sequence. Sedimentary Geology 155, 301–316.

Harris, D. L. (1963), Characteristics of the hurricane storm surge, Tech. Pap. 48, U. S. Weather Bur., Washington, D. C., 139 pp.

Haque, C.E., 1997. Atmospheric hazards preparedness in Bangladesh: a study of warning, adjustments and recovery from the April 1991 cyclone, in: Earthquake and Atmospheric Hazards. Springer, pp. 181–202.

Heming, J.T., Chan, J.C.L., Radford, A.M., 1995. A new scheme for the initialisation of tropical cyclones in the UK Meteorological Office global model. Meteorological Applications 2, 171–184.

Hearn, C. J. (2008). The dynamics of coastal models. Cambridge University Press.

Holland, G.J., 1980. An analytic model of the wind and pressure profiles in hurricanes. Monthly weather review 108, 1212–1218.

Hydraulics, D., 2009. Delft3D-FLOW user manual. Delft, the Netherlands.

Ikeda K 1995. Gender differences in human loss and vulnerability in natural disasters: a case study from Bangladesh, Indian J Gen Stud 2(2):171 193.

Karim, M.F., Mimura, N., 2008. Impacts of climate change and sea-level rise on cyclonic storm surge floods in Bangladesh. Global Environmental Change 18, 490–500.

Knutson, T.R., McBride, J.L., Chan, J., Emanuel, K., Holland, G., Landsea, C., Held, I., Kossin, J.P., Srivastava, A.K., Sugi, M., 2010. Tropical cyclones and climate change. Nature Geoscience 3, 157–163.

McPhaden, M.J., Foltz, G.R., Lee, T., Murty, V.S.N., Ravichandran, M., Vecchi, G.A., Vialard, J., Wiggert, J.D., Yu, L., 2009. Ocean-atmosphere interactions during cyclone nargis. EOS, Transactions American Geophysical Union 90, 53–54.

Meehl, G.A., Covey, C., Delworth, T., Latif, M., McAvaney, B., Mitchell, J.F.B., Stouffer, R.J., Taylor, K.E., and. Coauthors, 2007: Global climate projections. Climate Change 2007: The Physical Science Basis, S. Solomon et al., Eds. Cambridge University Press.

Murty, T.S., Flather, R.A., Henry, R.F., 1986. The storm surge problem in the Bay of Bengal. Progress in Oceanography 16, 195–233.

Mukhopadhyay, A., Mondal, P., Barik, J., Chowdhury, S.M., Ghosh, T., Hazra, S., 2015. Changes in mangrove species assemblages and future prediction of the Bangladesh Sundarbans using Markov chain model and cellular automata. Environmental Science: Processes & Impacts 17, 1111–1117.

Milliman, John D., James M. Broadus, and Frank Gable. 1989 Environmental and economic implications of rising sea level and subsiding deltas: the Nile and Bengal examples. Ambio 340-345.

Mohal, N., Khan, Z.H., Rahman, N., 2006. Impact of sea level rise on coastal rivers of Bangladesh. Dhaka: Institute of Water Modelling (IWM). Assessment conducted for WARPO, an organization under Ministry of Water Resources.

Meehl, G.A., Covey, C., Delworth, T., Latif, M., McAvaney, B., Mitchell, J.F.B., Stouffer, R.J., Taylor, K.E., n.d. Coauthors, 2007: Global climate projections. Climate Change 2007: The Physical Science Basis, S. Solomon et al., Eds. Cambridge University Press

Nash, J.E., Sutcliffe, J.V., 1970. River flow forecasting through conceptual models part I—A discussion of principles. Journal of hydrology 10, 282–290.

Nicholls R J N, Mimura N, Topping J C 1995. Climate change in South and Southeast Asia: some implications for coastal areas, Journal of Global Environmental Engineering 1, 137-154.

Pietrafesa, L. J., Janowitz, G. S., Chao, T. Y., Weisberg, R. H., Askari, F., & Noble, E. 1986 The physical oceanography of Pamlico Sound. University of North Carolina Sea Grant Publication UNC-WP-86-5, Raleigh, North Carolina, 125

Pietrafesa, L.J., Bao, S., Yan, T., Slattery, M., Gayes, P.T., 2016. On Sea Level Variability and Trends in United States Coastal Waters and Relationships with Climate Factors. Advances in Adaptive Data Analysis 7, 1550005.

Sakib, M., Nihal, F., Haque, A., Rahman, M., Ali, M., 2015. Sundarban as a Buffer against Storm Surge Flooding. World Journal of Engineering and Technology 3, 59.

Shamsuddoha M and Chowdhury R K 2007: Climate Change Induced Forced Migrants: in need of dignified recognition under a new Protocol, Coastal Association for Social Transformation Trust (COAST Trust); Equity and Justice Working Group (EJWG), 2007, 32 p.

Sengupta, D., Goddalehundi, B.R., Anitha, D.S., 2008. Cyclone-induced mixing does not cool SST in the post-monsoon North Bay of Bengal. Atmospheric Science Letters 9, 1–6.

Singh, O.P., Khan, T.M.A., Rahman, M.S., 2001. Has the frequency of intense tropical cyclones increased in the north Indian Ocean? CURRENT SCIENCE-BANGALORE-80, 575–580.

SMRC, 2003. The Vulnerability Assessment of the SAARC Coastal Region due to Sea Level Rise: Bangladesh Case. SAARC Meteorological Research Center, Dhaka SMRC-No. 3.

Stocker, T.F., Qin, D., Plattner, G.K., Tignor, M., Allen, S.K., Boschung, J., Nauels, A., Xia, Y., Bex, B. and Midgley, B.M., 2013. IPCC, 2013: climate change 2013: the physical science basis. Contribution of working group I to the fifth assessment report of the intergovernmental panel on climate change.

Vatvani, D.K., Gerritsen, H., Stelling, G. S., Rao, A. K., 2002. Cyclone induced storm surge and flood forecasting system for India. Solutions to Coastal Disasters '02, San Diego, CA, 2002.

Warrick, R.A., Bhuiya, A.A.H., Mitchell, W.M., Murty, T.S., Rasheed, K.B.S., 1996. Sea-level Changes in the Bay of Bengal, in: The Implications of Climate and Sea–Level Change for Bangladesh. Springer, pp. 97–142.

Whitehead, P.G., Barbour, E., Futter, M.N., Sarkar, S., Rodda, H., Caesar, J., Butterfield, D., Jin, L., Sinha, R., Nicholls, R., others, 2015. Impacts of climate change and socio-economic scenarios on flow and water quality of the Ganges, Brahmaputra and Meghna (GBM) river systems: low flow and flood statistics. Environmental Science: Processes & Impacts 17, 1057–1069.

Xie, L., Bao, S., Pietrafesa, L.J., Foley, K., Fuentes, M., 2006. A real-time hurricane surface wind forecasting model: Formulation and verification. Monthly Weather Review 134, 1355–1370.

Zhang, K., Liu, H., Li, Y., Xu, H., Shen, J., Rhome, J., Smith, T.J., 2012. The role of mangroves in attenuating storm surges. Estuarine, Coastal and Shelf Science 102, 11–23.